



**HAL**  
open science

## Quantitative analysis of electronic absorption of phosphorus donors in diamond

I. Stenger, Marie-Amandine Pinault-Thaury, Alain Lusson, Thierry Kociniewski, François Jomard, Jacques Chevallier, Julien Barjon

► **To cite this version:**

I. Stenger, Marie-Amandine Pinault-Thaury, Alain Lusson, Thierry Kociniewski, François Jomard, et al.. Quantitative analysis of electronic absorption of phosphorus donors in diamond. *Diamond and Related Materials*, 2017, 74, pp.24-30. 10.1016/j.diamond.2017.01.012 . hal-02440909

**HAL Id: hal-02440909**

**<https://hal.science/hal-02440909>**

Submitted on 27 Jan 2021

**HAL** is a multi-disciplinary open access archive for the deposit and dissemination of scientific research documents, whether they are published or not. The documents may come from teaching and research institutions in France or abroad, or from public or private research centers.

L'archive ouverte pluridisciplinaire **HAL**, est destinée au dépôt et à la diffusion de documents scientifiques de niveau recherche, publiés ou non, émanant des établissements d'enseignement et de recherche français ou étrangers, des laboratoires publics ou privés.

1 Quantitative analysis of electronic absorption of phosphorus donors in  
2 diamond

3  
4 I. Stenger, M.-A. Pinault-Thaury, A. Lusson, T. Kociniewski, F. Jomard, J. Chevallier and J.  
5 Barjon

6  
7 Université Paris Saclay, Université St Quentin Yvelines, CNRS, GEMaC  
8 45 avenue des Etats Unis, 78035 Versailles Cedex, France

9  
10 \*corresponding author  
11 +33 (0)1 39 25 46 71 / (ingrid.stenger@uvsq.fr, I. Stenger)

12  
13 **ABSTRACT**

14 In this work, phosphorus donors in diamond have been investigated by means of Fourier  
15 Transform Infra-Red (FTIR) transmission spectroscopy on a series of fully-characterized  
16 homoepitaxial layers. Low-temperature FTIR absorption spectra have been obtained for  
17 concentrations of donors in the range  $N_D = 3.7 \times 10^{16} - 3.5 \times 10^{18} \text{ cm}^{-3}$  and compensating  
18 acceptor impurities in the range  $N_A = 2.3 \times 10^{16} - 3.0 \times 10^{18} \text{ cm}^{-3}$ . The absorption spectra is  
19 shown to exhibit two peaks at  $4220 \text{ cm}^{-1}$  and  $4540 \text{ cm}^{-1}$  corresponding to electronic transitions  
20 from the ground state to the  $2p_0$  and  $2p_{+/-}$  excited states, respectively, of phosphorus donors in  
21 the neutral state of charge. The intensity of the most intense peak at  $4540 \text{ cm}^{-1}$  is found  
22 proportional to  $N_D - N_A$  over two decades. The absorption cross-section of the corresponding  
23 transition is deduced providing a calibration law for the determination of  $N_D - N_A$  in phosphorus-  
24 doped diamond. Furthermore, the linewidth of the peak exhibits a linear variation with the  
25 compensating acceptor concentration, interpreted as the effect of the distribution of ionized  
26 impurities. The use of the non-destructive and contact-less FTIR optical method is finally  
27 discussed to determine the compensation ratio in phosphorus-doped diamond.

28  
29 **Keywords** : Infrared absorption, n-type diamond, diamond impurities, wide bandgap  
30 semiconductor

## I. INTRODUCTION

The n-type conductivity in diamond is presently one of the major issues for electronic applications such as high power devices, UV light emitting diodes, DNA sensors, and electron emitters [1,2,3,4,5,6]. Up to now phosphorus is the substitutional donor which gives the highest n-type conductivities, despite its high ionization energy of 0.6 eV [7]. Using microwave-plasma-assisted chemical vapour deposition (MPCVD), phosphorus can be incorporated in substitutional sites of the diamond lattice during the growth. Its incorporation remains easier on (111) oriented diamond surfaces than on (100) [8,9] though this surface is preferred for applications. However, both (111) and (100) homoepitaxial layers still suffer from a relatively high compensation of donors by residual impurities and defects [10]. Today, it is striking that the n-type conductivity of phosphorus-doped diamond at room temperature is mainly limited by the problem of compensation rather than by the donor concentration. Up to now, the lowest compensation ratios, defined as  $k=N_A/N_D$ , ( $N_A$  the compensating acceptor concentration and  $N_D$  the donor concentration) reported in n-type diamond are ~40% on the (100) orientation [11] and ~5 % on the (111) orientation [12], as deduced from electrical measurements. The contrast is striking with p-type diamond doped with boron where the compensation ratio can reach values below one part per million [13].

Evaluating the compensation ratio of phosphorus-doped diamond by Hall effect measurements is not an easy task because of the high resistivity of the films and the high contact resistance of metals on n-type diamond. Cathodoluminescence (CL) spectroscopy has proven [14] to be a powerful optical technique to quantify the concentration of phosphorus incorporated in donor sites,  $N_D$ . However, under electron-hole pair injection, all acceptors are neutralized. Consequently, the compensation effect is not assessed with CL spectroscopy.

1           An alternative technique to probe the phosphorus donors in diamond is infrared  
2 absorption spectroscopy. It is commonly used for a quantitative analysis of impurity  
3 concentrations in semiconductors from the knowledge of the absorption cross-section of  
4 electronic or vibrational transitions [15]. For p-type diamond doped with boron, Collins *et al*  
5 correlated the absorption intensity of the electronic transitions of neutral boron to its  
6 concentration and provided calibration curves [16]. In 2000, electronic transitions between the  
7 ground state  $1s$  and different excited states of neutral phosphorus atoms were observed by  
8 infrared absorption spectroscopy by Gheeraert *et al*. The authors discussed the photoionization  
9 background and related its magnitude to the phosphorus content in the gas mixture during  
10 growth [17]. However, the lack of accurate values of  $N_D$  and  $N_A$  in their samples prevent them  
11 to give a more useful calibration law for phosphorus-doped diamond characterization.

12           In this work, we have chosen to focus on the  $1s \rightarrow 2p_{\pm}$  absorption peak at  $4540 \text{ cm}^{-1}$  since  
13 it is the most intense absorption line associated to the electronic transitions of phosphorus  
14 donors in diamond. The infrared absorption measurements have been performed in a series of  
15 extensively characterized homoepitaxial layers with different phosphorus doping levels. We  
16 demonstrate that the intensity of the electronic absorption of phosphorus donors at  $4540 \text{ cm}^{-1}$  is  
17 proportional to the net donor density, namely  $N_D - N_A$ . We provide a calibration curve for the  
18 measurement of  $N_D - N_A$  by using infrared spectroscopy. We also observe that the linewidth of  
19 the  $1s \rightarrow 2p_{\pm}$  absorption peak follows a linear dependency on  $N_A$ . The possible origins of the  
20 broadening are discussed. We further evaluate the uncertainty associated to the determination  
21 of the compensation from infrared measurements, performed alone or in a combination with  
22 other techniques, such as CL or Secondary Ion Mass Spectrometry (SIMS).

23

24

## II. EXPERIMENTS

1  
2  
3  
4  
5  
6  
7  
8  
9  
10  
11  
12  
13  
14  
15  
16  
17  
18  
19  
20  
21  
22  
23

The (111) and (100) phosphorus doped homoepitaxial diamond films were grown on type Ib diamond crystals by microwave plasma assisted chemical vapor deposition (MPCVD). For the (111) orientation, the deposition conditions were described by Kociniewski *et al* [18, 19]. The D147 and D166 samples are replicas of the D42 sample, with  $N_D$  of the same order of magnitude. The (100) oriented sample was grown thanks to the new set of growth parameters we found recently [20].

Secondary-ion mass spectrometry experiments (SIMS) using a Cameca IMS 4f equipment were performed onto the samples in order to measure the depth distribution of P, B, N, H atoms into the diamond films, with  $Cs^+$  primary ions accelerated at 10 keV. **In most of the samples, a single SIMS crater of approximately  $150 \times 150 \mu m^2$  was dug at sample edges ( $2 \times 2 mm^2$  or  $3 \times 3 mm^2$ ).** The concentrations of P and B were quantified by using implanted standards. As shown in our previous papers, the phosphorus concentration of our epilayers is quite homogeneous both in depth and laterally [19]. Nevertheless, for each sample, we present the mean value of the SIMS profile on the whole layer thickness. The hydrogen and nitrogen concentrations are at the SIMS level detection limit while the residual boron concentration (contamination) is in the range  $1.5-6 \times 10^{16} cm^{-3}$ , well below the P concentration. The P concentration ranged from  $3.7 \times 10^{16} at.cm^{-3}$  to  $3.5 \times 10^{18} at.cm^{-3}$  and the thickness of the epilayers ranged from 1 to 6.3  $\mu m$ . The relative uncertainties are estimated at 10% both for the P concentration and the film thickness.

The DC electrical measurements were performed by resistivity and Hall effect in a van der Pauw configuration from 300 K to 900 K under a DC magnetic field of 0.8 T, with a high impedance setup. The Hall scattering factor is assumed to be equal to 1. Prior to the electrical

1 measurements, the as-grown diamond film surfaces were oxidized in order to remove the  
2 surface conductive layer due to the hydrogen termination (see ref. [18] for details).

3 Capacitance - voltage measurements were performed on the (100) oriented sample to  
4 determine the neutral donor concentration profile  $N_D - N_A$  in the first 500 nm of the film (see  
5 ref [11] for details), with a relative uncertainty estimated at 10%.

6 Infrared transmission spectra were recorded from 1800 to 8500  $\text{cm}^{-1}$  in a BOMEM DA8  
7 Fourier Transform Infrared interferometer. Liquid nitrogen or liquid helium were used to cool  
8 down the samples at temperatures ranging from 10 K to 250 K. A globar light source and a  
9 InSb detector were used. The spectral resolution was set to 4  $\text{cm}^{-1}$ . The transmission was  
10 normalized to  $T/T_0=1$  at 4000  $\text{cm}^{-1}$  where the absorption of neutral phosphorus vanishes ( $T$ :  
11 sample transmission and  $T_0$ : sample transmission at 4000  $\text{cm}^{-1}$ ). The absorption coefficient was  
12 then found from the usual relationship:  $\alpha = -\frac{1}{d} \ln\left(\frac{T}{T_0}\right)$ ,  $d$  being the film thickness obtained from  
13 SIMS analysis.

### 14 III. RESULTS AND DISCUSSION

#### 15 A. Compensation ratio and neutral donor concentration

16 As a result of the almost complete substitutional incorporation of phosphorus in (111)  
17 epilayers [21] and also in the (100) epilayer we have investigated [20], we consider that all  
18 phosphorus atoms incorporated in diamond in the series of samples act as donors. In other  
19 words, phosphorus are located in substitution of carbon atoms and are not complexed with other  
20 impurity or defects (ex : H or V). Consequently, we will assume that the phosphorus  
21 concentration deduced from SIMS experiments equals the concentration of donors ( $N_D$ ).

22 From Hall effect measurements as a function of temperature, we deduce the  
23 compensation ratio  $k=N_A/N_D$  for the (111) oriented samples by using the procedure described  
24 in ref. [22]. The equivalent density of states effective mass was updated to  $m_c^*=1.639m_0$

1 following the work of Naka et al. [23]. It follows a slightly different value of  $k$  comparing to  
 2 those found in ref. 22. The relative uncertainty is estimated at  $\Delta k/k=20\%$ . For the (100) oriented  
 3 sample D169b, the compensation ratio was determined by combining : (i) the neutral donor  
 4 concentration  $N_D-N_A$  extracted from  $C(V)$  measurements on the first 500 nm of the film<sup>1</sup> and  
 5 (ii) the donor concentration  $N_D$  measured by SIMS on the same part of the film. We then  
 6 assumed that  $k$  is constant in the entire thickness of the film. The sample characteristics are  
 7 summarized in Table I <sup>2</sup>.

8 TABLE I. Sample characteristics. Phosphorus donor concentrations ( $N_D$ ) from SIMS, thickness  
 9 ( $d$ ), compensation ratio ( $k$ ) deduced from electrical measurements and the corresponding  
 10 concentrations of compensating acceptors ( $N_A$ ) and neutral phosphorus donors ( $N_D-N_A=(1-$   
 11  $k)N_D$ ), integrated intensity ( $I_A$ ) and full width at half maximum ( $\Gamma$ ) of the  $1s \rightarrow 2p_{\pm}$  absorption  
 12 peak. Sample D169b is (100)-oriented. All others are (111)-oriented.

Sample ref.	$N_D$ (cm <sup>-3</sup> )	$d$ ( $\mu$ m)	$k$ (%)	$N_A$ (cm <sup>-3</sup> )	$N_D-N_A$ (cm <sup>-3</sup> )	$I_A$ (cm <sup>-2</sup> )	$\Gamma$ (cm <sup>-1</sup> )
D169b	$3.7 \times 10^{16}$	6.30	40	$1.5 \times 10^{16}$	$2.3 \times 10^{16}$	75	15
D46	$6 \times 10^{17}$	1.32	34	$2.0 \times 10^{17}$	$4.0 \times 10^{17}$	1777	25
D43	$8.5 \times 10^{17}$	1.62	34	$2.9 \times 10^{17}$	$5.6 \times 10^{17}$	3031	31
D48	$9.4 \times 10^{17}$	1.46	14	$1.3 \times 10^{17}$	$8.1 \times 10^{17}$	2668	23
D42	$1.7 \times 10^{18}$	1.23	9	$1.5 \times 10^{17}$	$1.5 \times 10^{18}$	5160	26
D31	$3.0 \times 10^{18}$	1.50	35	$1.1 \times 10^{18}$	$2.0 \times 10^{18}$	--	64
D147	$3.5 \times 10^{18}$	1.12	16	$5.7 \times 10^{17}$	$3.0 \times 10^{18}$	10403	44
D166	$3.5 \times 10^{18}$	1.52	21	$7.4 \times 10^{17}$	$2.8 \times 10^{18}$	9500	39

13  
 14 Let us discuss the origin of compensation in our n-type diamond layers. Residual boron  
 15 acceptors are naturally compensating centers.  $[B]/[P]$  is less than 3% in all the samples and is

<sup>1</sup> The achievement of ohmic contact is an issue in n-type diamond. At low doping, metallic layers usually gives rectifying-contact characteristics which impede Hall measurements. That's the reason why  $C(V)$  was used instead of Hall for the D169b sample which has the lightest doping.

<sup>2</sup> In the case of D169b which is a relatively thick layer, the phosphorus concentration varies along the layer (SIMS profile can be found in ref.20). The concentration given in ref [20] and [11] are averaged on the first 800 nm of the layer. This is the correct method to compare the impurity concentration with surfacic measurements such as a  $C(V)$  measurement or cathodoluminescence at low voltage. As FTIR absorption occurs in the whole film thickness, it is necessary to indicate the mean  $N_D$  concentration over the total depth of the layer in table I.

1 therefore much lower than  $k$ . As a result, the compensation of phosphorus donors is not limited  
2 by the presence of residual boron atoms in n-type diamond. Other residual impurities and/or  
3 defects reduce the phosphorus electrical activity. In high quality CVD diamond, the  
4 contamination with other elements (N, Si, ...) would be almost negligible if enough care is  
5 taken in the growth process. P-H and P-V are possible compensating complexes in n-type  
6 diamond [24, 25, 26, 27]. However, they are expected to be in negligible concentration because  
7 100% of the P atoms act as substitutional donors in our homoepitaxial layers. The hydrogen-  
8 multi vacancy complexes  $V_n-H_n$  are other possible compensators of phosphorus donors. Some  
9 of them were identified and could act as compensators: H1, H2 [28], VH [29] and H1' [30].  
10 The H1' center should be dominant in diamond epitaxy. Being often observed in undoped and  
11 boron-doped CVD diamond by electron spin resonance (ESR) [28], this hydrogen-vacancy  
12 complex presents a carbon dangling bond near a hydrogen atom. Note that extended defects  
13 specific to growth (e.g. dislocations) could also participate to the compensation of phosphorus  
14 donors. As a summary, the identification of compensating defects in phosphorus doped  
15 diamond remains an issue to be solved.

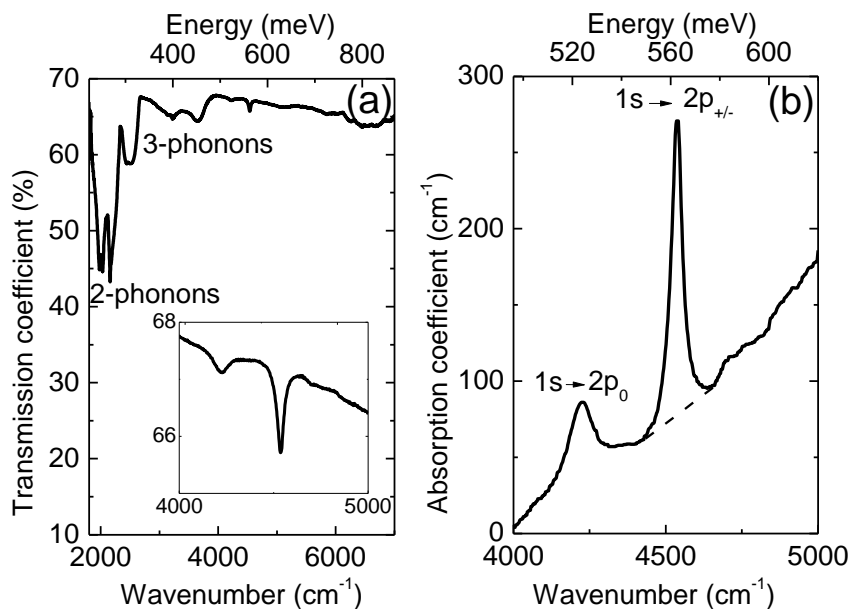
## 16 **B. Electronic transitions of neutral phosphorus donors in diamond**

17 A transmission spectrum at 10K of a  $3.5 \times 10^{18}$  at.cm<sup>-3</sup> P-doped film (sample D147) is  
18 plotted in figure 1(a). From 1800 cm<sup>-1</sup> to 4000 cm<sup>-1</sup>, it exhibits typical features corresponding  
19 to intrinsic absorption from diamond involving 2-phonons and 3-phonons lattice absorption  
20 bands [31]. At approximately 2800 cm<sup>-1</sup>, peaks associated to C-H vibrations could be classically  
21 observed, as well as H<sub>2</sub>O artifacts at 3000 cm<sup>-1</sup>. The box presents a magnification of the 4000  
22 cm<sup>-1</sup>-5000 cm<sup>-1</sup> spectral range in which the signature of electronic transitions of neutral  
23 phosphorus donors are expected.

24 The absorption coefficient at 10 K of sample D147 is plotted in figure 1(b). It exhibits  
25 a continuous background due to the photoionization continuum and two peaks attributed to the



1 transitions from the ground level  $1s$  to the  $2p_0$  and  $2p_{\pm}$  excited states respectively at  $4220 \text{ cm}^{-1}$   
 2 ( $523 \text{ meV}$ ) and  $4540 \text{ cm}^{-1}$  ( $562 \text{ meV}$ ). Interestingly, Gheeraert *et al.* compared the positions of  
 3 the peaks to the results of the Effective Mass Approximation (EMA) [32]. While the excited  
 4 state energies of the phosphorus donor in diamond are well described in the EMA theory, it  
 5 fails to describe the ground state energy. The experimental ionization energy of phosphorus is  
 6  $0.6 \text{ eV}$  to be compared with  $0.19 \text{ eV}$  for a hydrogenic donor in diamond. (This last value was  
 7 updated with the effective masses of ref [23] using the EMA theory described in details in ref  
 8 [33]). Such a discrepancy indicates that the wave function of the weakly bound electron of the  
 9 donor in its ground state is much strongly localized in the real space than predicted with the  
 10 EMA theory. Butorac *et al.* have indeed calculated the charge density along a P-C bond from  
 11 the density functional theory [34]. Their work shows that the phosphorus extra electron is  
 12 strongly localized around the phosphorus : the maximum of the charge density is found at only  
 13  $1.4 \text{ \AA}$  between phosphorus and its four nearest carbon neighbors. In the discussion of Part D,  
 14 we will use this value as an effective Bohr radius  $a^* = 1.4 \text{ \AA}$  for phosphorus donors in diamond.

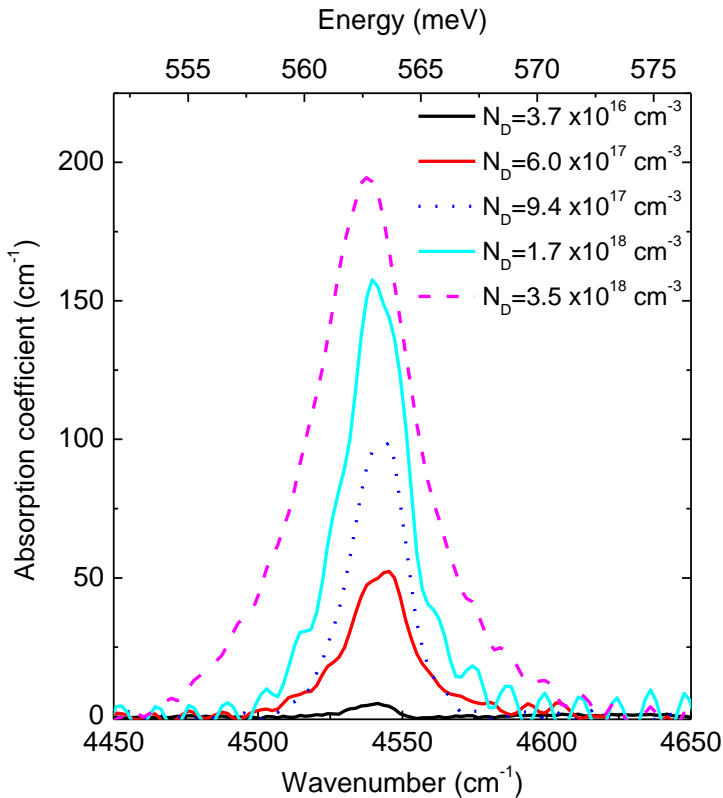


15

1 Fig. 1 : (a) Transmission spectrum of sample D147 containing  $3.5 \times 10^{18} \text{ P.cm}^{-3}$ . (b)  
 2 Absorption spectrum of sample D147 showing the electronic transitions of neutral phosphorus  
 3 in n-type diamond. A background line has been drawn in for the  $4540 \text{ cm}^{-1}$  band.

### 4 C. Integrated absorption cross-section of neutral phosphorus donors

5 Figure 2 shows a set of spectra at 10 K centred on the  $1s \rightarrow 2p_{\pm}$  peak taken from diamond  
 6 layers with different phosphorus contents. The photoionization continuous background has  
 7 been subtracted. The general trend is that the intensity of absorption increases when increasing  
 8 the phosphorus concentration in diamond. After background subtraction, the integrated  
 9 intensity,  $I_A$ , and the full width at half maximum (FWHM),  $\Gamma$ , of the  $1s \rightarrow 2p_{\pm}$  absorption peak  
 10 of the phosphorus-doped diamond layers at 10 K, were extracted from a fit by using a Voigt  
 11 profile. The results are reported in Table 1.



12

1 Fig. 2 (color on line): Absorption coefficient at the  $1s \rightarrow 2p_{\pm}$  electronic transition of neutral  
2 phosphorus donors in diamond at 10K. It increases monotonically with the donor concentration  
3 in the homoepitaxial layer.

4 The integrated intensity of the  $1s \rightarrow 2p_{\pm}$  absorption peak is plotted as a function of the net donor  
5 concentration,  $N_D - N_A$ , in Figure 3. The net donor concentration corresponds to the part of  
6 donors which are not compensated by residual acceptors (also mentioned as the  
7 ‘uncompensated’ donor concentration). We observe that the integrated intensity is proportional  
8 to  $N_D - N_A$  over two decades. This important result is discussed in the following.

9         The  $1s \rightarrow 2p_{\pm}$  transition at  $4540 \text{ cm}^{-1}$  is attributed to neutral phosphorus donors. The  
10 intensity of this absorption line is then expected to be proportional to  $N_D^0$ . At low temperatures,  
11 donors are frozen. In other words, their excess electron remains bound to phosphorus, instead  
12 of feeding the conduction band with delocalized free electrons. In the absence of residual  
13 acceptors, all phosphorus atoms are expected to be neutral at low temperature. However, in the  
14 presence of residual acceptors at a concentration  $N_A < N_D$ , part of donors give their excess  
15 electron to acceptors, resulting in the full ionization of the latter,  $N_A = N_A^-$ . This describes the  
16 compensation phenomenon that occurs at thermodynamic equilibrium, whatever be the crystal  
17 temperature. In this process, a part of donors is also ionized ( $N_D^+ = N_A^-$ ), and the neutral donor  
18 concentration is then reduced to  $N_D^0 = N_D - N_A$ . This explains why the amplitude of the absorption  
19 coefficient at the  $1s \rightarrow 2p_{\pm}$  energy is strictly proportional to the net donor density  $N_D - N_A$  in the  
20 phosphorus-doped diamond samples (slope=1.0 in the  $\text{Ln}(I_A)$  vs  $\text{Ln}(N_D - N_A)$  plot). As a result,  
21 the infrared spectroscopy of phosphorus in diamond has a strong potential to investigate the  
22 compensation phenomenon in n-type diamond.

23         Fig. 3 can be further considered as a calibration curve for future measurements of  $N_D -$   
24  $N_A$  by infrared absorption. From it, we deduce the relationship (1) at 10 K. For the case of

1 experiments using liquid nitrogen cryostats, we also provide the relationship (2) measured at  
2 90 K using the same procedure.

3

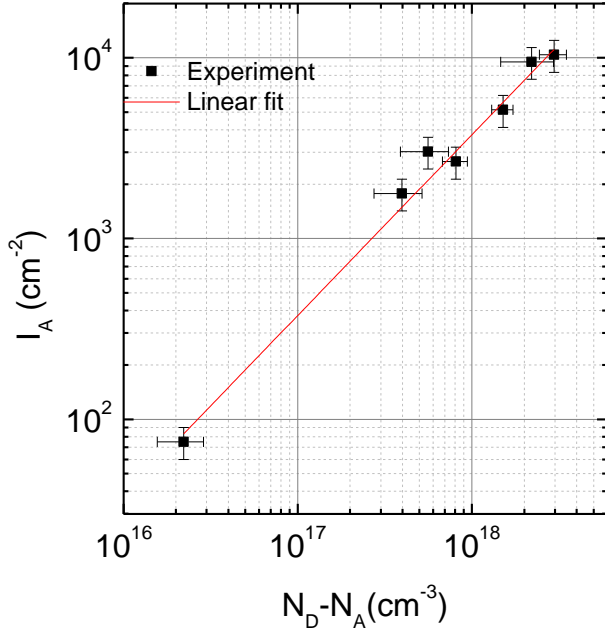
$$4 \quad N_D - N_A(\text{cm}^{-3}) = (2.7 \pm 0.2) \times 10^{14} \cdot I_A(\text{cm}^{-2}) \quad \text{at 10 K} \quad (1)$$

$$5 \quad N_D - N_A(\text{cm}^{-3}) = (4.2 \pm 0.5) \times 10^{14} \cdot I_A(\text{cm}^{-2}) \quad \text{at 90 K} \quad (2)$$

6 Let us discuss the error bars of Fig. 3 and the uncertainties associated to equation (1) in  
7 this paragraph. Considering  $N_A = kN_D$ , we deduce  $\Delta N_A/N_A = \Delta k/k + \Delta N_D/N_D = 30\%$ . The  
8 uncertainty on  $N_D - N_A$  is then equal to  $\Delta(N_D - N_A) = 0.1N_D + 0.3N_A$ , formula used to plot the error  
9 bars related to  $N_D - N_A$  in Fig. 3. Concerning the absorption integrated intensity  $I_A$ , we consider  
10  $\Delta I_A/I_A = 20\%$  including a relative uncertainty of 10% for the thickness of the epilayer. For  
11 sample D169b, the uncertainty is larger due to a lower signal to noise ratio. Eq. 1 and the  
12 associated uncertainty on the proportionality factor is the result of a least mean-square linear fit  
13 of  $I_A$  as a function of  $N_D - N_A$  weighted by the error bars introduced in this paragraph. Finally,  
14 the relative uncertainty on  $N_D - N_A$  when using Eq. 1 is estimated at 27 %.

15 Note that the detection limit for the FTIR absorption of phosphorus in diamond is mainly driven  
16 by the product of the concentration of absorbing impurities times film thickness. With our setup  
17 and a typical integration time of 2 minutes, we experience a detection limit of approximately

$$18 \quad N_D - N_A (\text{cm}^{-3}) = 1 \times 10^{17} / d(\mu\text{m})$$



1

2 Fig. 3 : Integrated intensity of the  $1s \rightarrow 2p_{\pm}$  transition related absorption peak at 10 K versus the  
 3 neutral phosphorus donor concentration. D31 sample was excluded from Fig. 3 because of too  
 4 many SIMS craters<sup>3</sup>.

5

#### D. Broadening of the $1s \rightarrow 2p_{\pm}$ transition

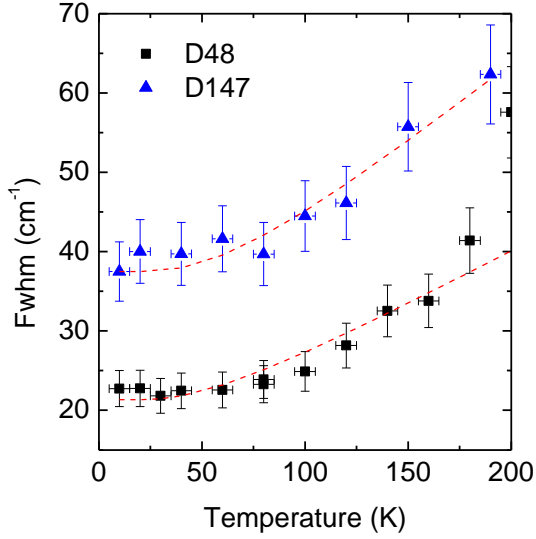
6

7 The linewidth (full width at half maximum) of the absorption peak is also worth  
 8 investigating. In Table I, one can observe strong variations of the linewidth  $\Gamma$  of the  $1s \rightarrow 2p_{\pm}$   
 9 absorption peak in the series of samples, from  $15 \text{ cm}^{-1}$  to  $64 \text{ cm}^{-1}$ . From our series of n-type  
 10 diamond samples, we found  $15 \text{ cm}^{-1}$  for the narrowest peak. This is lower than the linewidth  
 11 previously reported in ref [35] ( $23 \text{ cm}^{-1}$ ), this is a good indication of the high quality of the  
 12 layers. In Fig. 4, we have plotted the linewidth  $\Gamma$  as a function of (a)  $N_D$ , (b)  $N_D - N_A$  and (c)  $N_A$ .  
 13 We observe that the linewidth almost follows a linear variation with  $N_A$ , whereas it is clearly  
 not the case for  $N_D$  or  $N_D - N_A$ .

---

<sup>3</sup> Concerning sample D31, it contains SIMS craters in the middle of the sample performed for a reproducibility experiments, so we decided to exclude the FTIR intensity from our study. Nevertheless, it is still an interesting sample which acceptor concentration is the highest of our series of samples. Note that a FTIR absorption spectrum of D31 can be found in [19] prior to the homogeneity study and confirms the large FWHM of the peak.

1 In semiconductors, several effects are known to potentially broaden the electronic  
 2 absorption transitions of doping impurities: (i) the phonon lifetime broadening due to the  
 3 electron phonon interaction [36, 37] (ii) the overlap between impurity wavefunctions [38] ; (iii)  
 4 strain and inhomogeneities induced by defects and impurities [39,40] ; (iv) the presence of  
 5 random electric fields arising from ionized impurities [41,42,43].



6  
 7 Fig. 4: Full width at half maximum of the  $1s \rightarrow 2p_{\pm}$  absorption peak as a function of temperature  
 8 for samples D48 and D147.

9 Starting with the phonon-induced broadening (i), it is expected to occur at high  
 10 temperatures where the phonon population is significant. This is the reason why the linewidth  
 11 of the  $1s \rightarrow 2p_{\pm}$  absorption peak was measured as a function of temperature. To give examples,  
 12 it has been plotted in Fig. 4 for samples D48 and D147. We determine the characteristic  
 13 temperature  $T_c$  above which electron-phonon interaction becomes predominant. We use the  
 14 phenomenological expression, proposed by Barrie and Nishikawa [44]:

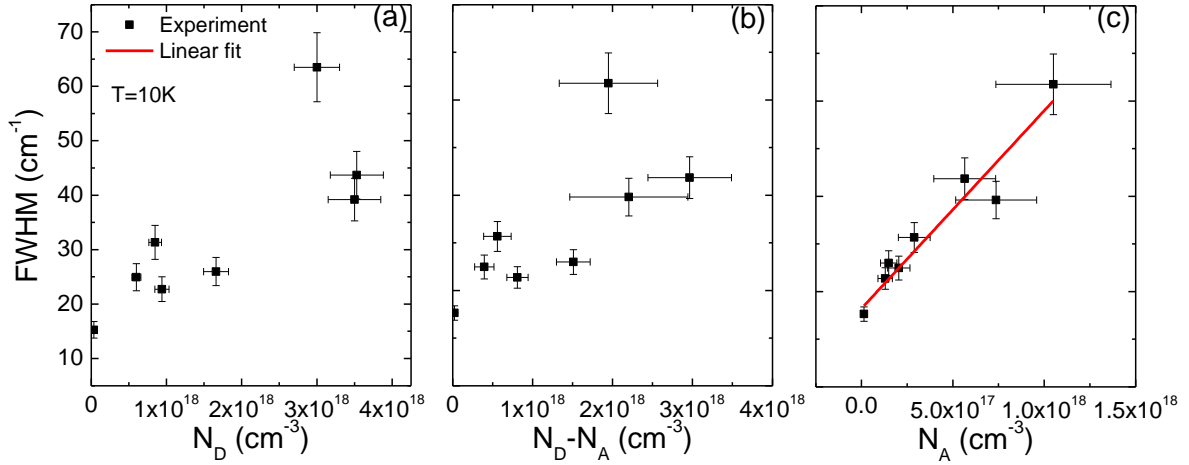
$$15 \quad \Gamma = \frac{\Gamma_{0K}}{1 - \exp(-T_c/T)} \quad (2)$$

16 where  $\Gamma_{0K}$  is the linewidth at 0 K and  $T_c$  is the critical temperature. Setting these two parameters  
 17 as adjustment parameters in a chi-square minimization procedure, the phenomenological

1 equation (2) appears to well describe the temperature dependence of the linewidth observed  
2 experimentally. From the fit, we found  $T_c=177\text{K}$  for sample D147 and  $T_c=151\text{K}$  for sample  
3 D48. These critical temperatures are much higher than 10K. As a result, the broadening due to  
4 phonon interactions is negligible at 10K.

5 In the next paragraphs, we propose to review the order of magnitudes of the other effects  
6 (ii-iv) in the case of phosphorus-doped diamond assuming a 1s level associated with the  
7 effective Bohr radius,  $a^*=1.4 \text{ \AA}$ , introduced previously. We insist on the fact that the ground  
8 level of phosphorus donors in diamond cannot be described as a pure 1s level according to the  
9 EMA theory. Still, the introduction of an effective Bohr radius makes possible to evaluate the  
10 order of magnitudes of these effects in phosphorus doped diamond.

11 Concerning the donor wavefunction overlapping (ii), Baltensberger's calculations of the 1s,  
12 2s, 2p bands for a lattice of hydrogen-like impurities [45] show that the broadening of the  
13 fundamental state becomes important when  $r_s \approx 6a^*$ , with  $a^*$  the effective Bohr radius of the  
14 bound carrier in a crystal with dielectric constant  $\epsilon$ .  $r_s$  is defined by  $4\pi r_s^3/3=1/N_D$ . Actually,  
15 following the approach of Ref. [45] and using  $a^*=1.4\text{\AA}$ , the broadening of donor levels would  
16 only occur at concentrations above  $4 \times 10^{20} \text{ P.cm}^{-3}$ . This is consistent with Fig. 5(a) and Fig. 5(b),  
17 where the linewidth  $\Gamma$  are plotted as a function of  $N_D$  and  $N_D-N_A$  respectively. No linear  
18 variation of  $\Gamma$  with  $N_D$  nor  $N_D-N_A$  is observed. This evidences that  $N_D$  is not the parameter  
19 governing the broadening of the absorption peak in the investigated series of diamond epilayers  
20 having  $3.5 \times 10^{18} \text{ P.cm}^{-3}$  at maximum.



1

2 Fig. 5 : Full width at half maximum (linewidth  $\Gamma$ ) at 10 K of the  $1s \rightarrow 2p_{\pm}$  absorption peak as a  
 3 function of (a) the phosphorus donor concentration (b) the neutral phosphorus donor  
 4 concentration (c) the acceptor concentration. All numerical values are given in Table I.

5 The broadening due to the random strain (iii) coming from the presence of defects and  
 6 impurities (iii) is also unlikely. The impurity-induced broadening should be proportional to their  
 7 total concentration in the crystal, which is not in agreement with our observations in Fig 5.  
 8 Concerning dislocations, they give rise to internal strain that shifts the conduction band minima  
 9 and hence broadens the excited states which follow them. This effect is expected to have a  
 10 negligible contribution on the broadening of electronic transitions [40] at the low dislocation  
 11 densities of typically  $10^{4-5}$  lines.cm<sup>-2</sup> observed in homoepitaxial layers grown on HPHT  
 12 substrates.

13 The ionized impurities (iv) are then likely to govern the linewidth of electronic transitions.  
 14 As all acceptors are ionized at low temperature, the concentration of ionized impurities  
 15 (positively and negatively charged ones) is  $N_I = N_D^+ + N_A^- = 2N_A$ . In other semiconductors like Ge  
 16 [46], the presence of these charges is known to create an electric field distribution that perturbs  
 17 the electronic states of the neutral impurities. In the assumption of a 1s ground level, the  
 18 linewidth increases linearly with  $N_I$  when the quadrupole interaction is dominant [41, 42, 43].  
 19 The absorption lineshapes are then symmetrical, as observed in Fig. 2. Such behaviour is also



1 observed in our diamond samples (see Fig. 2). This effect of ionized impurities is also coherent  
 2 with our experimental results, namely an absorption linewidth which exhibits a linear  
 3 dependence on  $N_A = N_I/2$ .

4 Fig. 5(c) shows the linewidth  $\Gamma$  plotted as a function of  $N_A$ . We observe that the linewidth  
 5 almost follows a linear variation with  $N_A$ . This result is consistent with a broadening governed  
 6 by the presence of ionized impurities (iv), while all other effects (i)-(iii) appear negligible in  
 7 our experimental conditions. Our work suggests that the electric field produced by ionized  
 8 impurities widen the  $1s \rightarrow 2p_{\pm}$  transition of phosphorus donors.

9 As a perspective, the linewidth might provide a way to directly evaluate  $N_A$ , the  
 10 compensator concentration, in phosphorus doped diamond. To that end, in Fig.5(c) is plotted  
 11 the result of a linear fit using a least mean-square procedure, each point weighted by its error  
 12 bar ( $\Delta N_A/N_A = 30\%$  and  $\Delta \Gamma/\Gamma = 10\%$ ). From it, we deduce the following relationship at 10 K:

$$13 \quad N_A(\text{cm}^{-3}) = (2.3 \pm 0.2) \times 10^{16} \times (\Gamma - 15.3)(\text{cm}^{-1}) \quad (3)$$

14 Obviously, Eq. (3) is restricted to phosphorus-doped diamond with high acceptor  
 15 concentrations  $N_A > 1.6 \times 10^{16} \text{cm}^{-3}$ . For smaller acceptor concentrations, the minimum linewidth  
 16  $\Gamma_0 = 15.3 \text{ cm}^{-1}$  is reached. We also remind that Eq.3 would be only valid for donor concentrations  
 17  $N_D < 4.10^{20} \text{ cm}^{-3}$ , concentration at which wavefunction overlapping (ii) is expected to occur. In  
 18 the severe limits mentioned above, the relative uncertainty on  $N_A$  obtained by Eq.3 is estimated  
 19 at  $\Delta N_A/N_A = 20\%$ .

20 Does  $\Gamma_0$  represent the natural linewidth, also called the homogeneous broadening ? If yes,  $\Gamma_0$   
 21 would be an intrinsic value, independent of the sample. This would first deserve to be confirmed  
 22 on other samples. Moreover, the value  $\Gamma_0 = 15.3 \text{ cm}^{-1}$  (1.9 meV) reached in sample D169b<sup>4</sup>,  
 23 remains large compared to conventional semiconductors. For instance  $\Gamma_0 \lesssim 0.2 \text{ cm}^{-1}$  in silicon

---

<sup>4</sup> Note that the FWHM of D169b is not limited by the spectral resolution of the apparatus. The lowest width that our setup is capable of resolving is  $5 \text{ cm}^{-1}$ , at the resolution used in our study.

1 is reported for most of dopants [15]. However, the situation in wide bandgap semiconductors  
2 might be different, due to the deep character of their dopants. They are quite deep in diamond :  
3 0.6 eV for phosphorus donors and 0.37 eV for boron acceptors. The FWHM of the main  
4 electronic absorption of boron acceptors at  $2800\text{ cm}^{-1}$  in diamond was also found to reach a 14  
5  $\text{cm}^{-1}$  minimum value in sample B01 of ref [13] which exhibits a boron concentration of  $[B]=$   
6  $10^{16}\text{cm}^{-3}$  and a very low compensation ratio (below  $10^{-6}$ ). At this point, further research is  
7 needed to answer this open question and to establish whether other effects contribute or not to  
8 the minimum linewidth  $\Gamma_0$  reached in this work<sup>5</sup>.

### 9 E. How to evaluate the compensation ratio from infrared spectroscopy ?

10 We have shown in section C that we can determine  $N_D-N_A$  by infrared absorption with  
11 a relative uncertainty estimated at 27%. In this section, we discuss different methods to  
12 determine the compensation ratio  $k$  with the help of electronic absorption spectroscopy of  
13 phosphorus donors in n-type diamond. We will pay attention to the relative uncertainty on  $k$ .  
14 This is a rarely tackled issue, though combining different techniques can result in huge  
15 uncertainties.

16 If  $N_D-N_A$  is measured by FTIR with Eq. (1) and  $N_D$  is determined by another technique  
17 (CL or SIMS for instance), it is easy to show that  $\Delta k/k = [\Delta(N_D-N_A)/N_D-N_A + \Delta N_D/N_D](1-k)/k$ ,  
18 based on the expression  $N_D-N_A = (1-k)N_D$ . We obtain numerically:  $\Delta k/k=0.37(1-k)/k$  when  
19 using the SIMS and FTIR uncertainties presented before. It is important to notice that  $\Delta k/k$  is a  
20 decreasing function of  $k$ . So the higher the compensation ratio, the lower the uncertainty on the

---

<sup>5</sup> The  $2p_0$  peak was unambiguously observed on several samples but not on the lowest concentration ones. A broadening of the  $2p_0$  is also likely to occur but we were not able to evidence it.

1 determination of  $k$ . For instance, the uncertainty on  $k$  is only 4% for  $k=90\%$ . This method  
2 should be preferred for highly compensated films ( $k>60\%$ ).

3 In the limit of  $N_D < 4 \times 10^{20} \text{ cm}^{-3}$  and  $N_A > 10^{16} \text{ cm}^{-3}$ , we might use Eq. (1) and (3) to  
4 determine both  $N_D - N_A$  (integrated intensity of absorption) and  $N_A$  (linewidth of absorption) by  
5 using only FTIR. The compensation ratio  $k = N_A/N_D$  would be then assessed with an uncertainty  
6  $\Delta k/k = 0.27 - 0.1k$ , again a decreasing function of  $k$ . In this case,  $\Delta k/k$  ranges from 18% to 26%  
7 for  $k$  decreasing from 90% to 10%. This method is more accurate than the first one for samples  
8 with low compensation level. In other cases it could be advantageous to combine  $N_A$  determined  
9 by FTIR and  $N_D$  known by another technique, SIMS here to be specific. This would give the  
10 uncertainty on  $k$  of  $\Delta k/k = 30\%$ .

#### 11 **IV. CONCLUSION**

12 The absorption coefficient spectra of phosphorus-doped diamond exhibit two peaks at  
13  $4220 \text{ cm}^{-1}$  and  $4540 \text{ cm}^{-1}$  corresponding to the  $1s \rightarrow 2p_0$  and  $1s \rightarrow 2p_{\pm}$  transitions of phosphorus  
14 donors in the neutral state of charge. The energy difference between them is consistent with the  
15 results of the Effective Mass Approximation theory applied here with updated electron effective  
16 masses. The main result of this work concerns the intensity of the  $2p_{\pm}$ -related peak which is  
17 shown to be proportional to  $N_D - N_A$ , also called the net donor density. The integrated absorption  
18 cross-section of the transition was evaluated at 10 K and 90K, providing a direct way to evaluate  
19 the net donor density with a contact-less and non-destructive FTIR optical technique.

20 The linewidth of the peak is also shown to follow a linear dependence on  $N_A$ , which is consistent  
21 with the presence of ionized impurities in the crystal. Specific cases have been identified where  
22 infrared absorption – alone or in a combination with other techniques – could provide a  
23 measurement of the compensation ratio.



- 
- efficiency of diamond deep-ultraviolet light emitting diode, *Appl. Phys. Lett.* **99**, 061110 (2011).
- [7] S. Koizumi, M. Kamo, Y. Sato, H. Ozaki and T. Inuzuka, Growth and characterization of phosphorous doped {111} homoepitaxial diamond thin films, *Appl. Phys. Lett.* **71**, 1065 (1997).
- [8] H. Kato, S. Yamasaki, and H. Okushi, n-type doping of (001)-oriented single-crystalline diamond by phosphorus, *Appl. Phys. Lett.* **86**, 222111 (2005).
- [9] G. Frangieh, F. Jomard, M. A. Pinault and J. Barjon, Influence of tertiarybutylphosphine (TBP) addition on the CVD growth of diamond, *Phys. Stat. Sol. A* **206**, 1996 (2009).
- [10] H. Kato, J. Barjon, N. Habka, T. Matsumoto, D. Takeuchi, H. Okushi and S. Yamasaki, Energy level of compensator states in (001) phosphorus-doped diamond, *Diamond Relat. Mater.* **20**, 1016 (2011).
- [11] M-A. Pinault-Thaury, I. Stenger, F. Jomard, J. Chevallier, J. Barjon, A. Traore, D. Eon and J. Pernot, Electrical activity of (100) n-type diamond with full donor site incorporation of phosphorus, *Phys. Stat. Sol. A* **212**, 2454 (2015)
- [12] M. Katagiri, J. Isoya, S. Koizumi and H. Kanda, Lightly phosphorus-doped homoepitaxial diamond films grown by chemical vapor deposition, *Appl. Phys. Lett.* **85**, 6365 (2004).
- [13] J. Barjon, E. Chikoidze, F. Jomard, Y. Dumont, M. –A. Pinault-Thaury, R. Issaoui, O. Brinza, J. Achard, and F. Silva, Homoepitaxial boron-doped diamond with very low compensation, *Phys. Stat. Sol. A* **209**, 1750 (2012)
- [14] J. Barjon, P. Desfonds, M.-A. Pinault, T. Kociniewski, F. Jomard and J. Chevallier, Determination of the phosphorus content in diamond using cathodoluminescence spectroscopy, *J. Appl. Phys.* **101**, 113701 (2007)
- [15] B. Pajot, *Optical absorption of impurities and defects in semiconducting crystals*, Springer

- 
- [16] A. T. Collins and A. W. S. Williams, The nature of the acceptor centre in semiconducting diamond, *J. Phys. C* **4**, 1789 (1971)
- [17] E. Gheeraert, S. Koizumi, T. Teraji, H. Kanda and M. Nesladek, Electronic states of phosphorus in diamond, *Diam. Relat. Mat.* **9**, 948 (2000)
- [18] T. Kociniewski, MA Pinault, J. Barjon, F. Jomard, J. and C. Saguy, MOCVD doping technology for phosphorus incorporation in diamond: Influence of the growth temperature on the electrical properties, *Diamond Relat. Mater.* **16**, 815 (2007)
- [19] T. Kociniewski, J. Barjon, M.-A. Pinault, F. Jomard, A. Lusson, D. Ballutaud, O. Gorochoy, J.M. Laroche, E. Rzepka, J. Chevallier and C. Saguy, n-type CVD diamond doped with phosphorus using the MOCVD technology for dopant incorporation, *Phys. Stat. Sol. (a)* **203**, 3136 (2006)
- [20] M.-A. Pinault-Thaury, B. Berini, I. Stenger, E. Chikoidze, A. Lusson, F. Jomard, J. Chevallier, and J. Barjon, High fraction of substitutional phosphorus in a (100) diamond epilayer with low surface roughness, *Appl. Phys. Lett.* **100**, 192109 (2012)
- [21] M. Hasegawa, T. Teraji and S. Koizumi, Lattice location of phosphorus in n-type homoepitaxial diamond films grown by chemical-vapor deposition, *Appl. Phys. Lett.* **79**, 3068 (2001)
- [22] I. Stenger, M.-A. Pinault-Thaury, T. Kociniewski, A. Lusson, E. Chikoidze, F. Jomard, Y. Dumont, J. Chevallier and J. Barjon, Impurity-to-band activation energy in phosphorus doped diamond, *J. Appl. Phys.* **114**, 073711 (2013)
- [23] N. Naka, K. Fukai, Y. Handa, and I. Akimoto, Direct measurement via cyclotron resonance of the carrier effective masses in pristine diamond, *Phys. Rev. B* **88**, 035205 (2013)
- [24] J. P. Goss, R. Jones, M. I. Heggie, C. P. Ewels, P. R. Briddon and S. Oberg, Theory of hydrogen in diamond, *Phys. Rev. B* **65**, 115207 (2002)

- 
- [25] A. Mainwood and A. M. Stoneham, Stability of electronic states of the vacancy in diamond, *J. Phys.: Condens. Matter* **9**, 2453 (1997).
- [26] R. Jones, J. E. Lowther, and J. Goss, Limitations to n-type doping in diamond: The phosphorus-vacancy complex, *Appl. Phys. Lett.* **69**, 2489 (1996).
- [27] T. Miyazaki and S. Yamasaki, Ab initio energetics of phosphorus related complex defects in synthetic diamond, *Physica B* **376–377**, 304 (2006).
- [28] X. Zhou, G. D. Watkins, K. M. M. Rutledge, R. P. Messmer and S. Chawla, Hydrogen-related defects in polycrystalline CVD diamond, *Phys. Rev. B* **54**, 7881 (1996).
- [29] C. Glover, M. E. Newton, P. M. Martineau, S. Quinn, and D. J. Twitchen, Hydrogen Incorporation in Diamond: The Vacancy-Hydrogen Complex, *Phys. Rev. Lett.* **92**, 135502 (2004).
- [30] N. Mizuochi, H. Watanabe, H. Okushi, S. Yamasaki, J. Niitsuma, and T. Sekiguchi, Hydrogen-vacancy related defect in chemical vapor deposition homoepitaxial diamond films studied by electron paramagnetic resonance and cathodoluminescence, *Appl. Phys. Lett.* **88**, 091912 (2006).
- [31] A. M. Zaitsev, *Optical Properties of diamond*, Springer, p69-124
- [32] E. Gheeraert, N. Casanova, A. Tajani, A. Deneuville, E. Bustarret, J.A. Garrido, C.E. Nebel and M. Stutzmann, n-Type doping of diamond by sulfur and phosphorus, *Diamond Relat. Mat.* **11**, 289 (2002)
- [33] R.A. Faulkner, Higher Donor Excited States for Prolate-Spheroid Conduction Bands: A Reevaluation of Silicon and Germanium, *Phys. Rev.* **184**, 713 (1969)
- [34] B. Butorac, and A. Mainwood, Symmetry of the phosphorus donor in diamond from first principles, *Phys. Rev. B* **78**, 235204 (2008)
- [35] E. Gheeraert, N. Casanova, S. Koizumi, T. Teraji and H. Kanda, Low temperature excitation spectrum of phosphorus in diamond, *Diamond Relat. Mat.* **10**, 444 (2001)

- 
- [36] M. Lax and E. Burnstein, Broadening of Impurity Levels in Silicon, *Phys. Rev.* **100**, 592 (1955)
- [37] E. O. Kane, Phonon Broadening of Impurity Lines, *Phys. Rev.* **119**, 40 (1960)
- [38] B. I. Shklovskii and A. L. Efros, *Electronic Properties of doped Semiconductors*, Springer series in Solid-State Science, vol. 45, Springer, Berlin, p. 50
- [39] M. Kogan and T. M. Lifshits, Photoelectric Spectroscopy – A New Method of Analysis of Impurities in Semiconductors, *Phys. Stat. Sol. (a)* **39**, 11 (1977)
- [40] C. Jagannath, Z. W. Grabowski, and A. K. Ramdas, Linewidths of the electronic excitation spectra of donors in silicon, *Phys. Rev.* **B 23**, 2082 (1981)
- [41] S.M. Kogan and N. Van Lien, Stark broadening of spectral lines of hydrogenic impurities in lightly doped compensated semiconductors at low temperatures, *Sov. Phys. Semicond.* **15**, 44 (1981)
- [42] D. M. Larsen, Inhomogeneous Line Broadening in Donor Magneto-Optical Spectra *Phys. Rev. B* **8**, 535 (1973)
- [43] D. M. Larsen, Inhomogeneous broadening of the Lyman-series absorption of simple hydrogenic donors, *Phys. Rev. B* **13**, 1681 (1976)
- [44] R. Barrie and K. Nishikawa, Phonon broadening of impurity spectral lines: II. application to silicon, *Can. J. Phys.* **41**, 1823 (1963)
- [45] W. Baltensberger, *Philos. Mag* **44**, 1355 (1953)
- [46] K. M. Itoh, J. Muto, W. Walukiewicz, J. W. Beeman, E. E. Haller, Hyunjung Kim, A. J. Mayur, M. Dean Sciacca, A. K. Ramdas, R. Buczko, J. W. Farmer, and V. I. Ozhogin, Evidence for correlated hole distribution in neutron-transmutation-doped isotopically controlled germanium, *Phys. Rev. B* **53**, 7797 (1996)